

LOCAL OSCILLATOR INDUCED INSTABILITIES IN TRAPPED ION FREQUENCY STANDARDS*

G. John Dick

California Institute of Technology
Jet Propulsion Laboratory
4800 Oak Grove Drive
Pasadena, CA 91109

ABSTRACT

The trapped ion frequency source is one of a class of passive atomic frequency standards that necessarily use an ancillary frequency source to interrogate the atomic transition. For passive atomic sources such as Rubidium standards, ultimate long term performance of the source is not dependent on this local oscillator, except to the extent limited by feedback gain. For the trapped ion source this immunity to local oscillator phase noise is lost. In contrast to the Rubidium source, a sequential measurement procedure is used in which the signal from the local oscillator is sensed only some of the time. Since the local oscillator is only periodically sampled, certain short term fluctuations in the local oscillator frequency will give rise to long term fluctuations in the difference between the stabilized local oscillator frequency and that of the atomic absorption.

We have performed calculations of the influence of such phase noise fluctuations in the reference oscillator on the performance of the standard as a function of duty cycle for a local oscillator with frequency fluctuations showing a $1/f$ spectral density, as is typically shown by crystal Quartz oscillators for long measuring times (1-100 seconds). Expressions are generated for the limiting trapped ion $\tau^{-1/2}$ variance due to the local oscillator for various values for the duty factor d . Explicitly treated are the cases $d \ll 1$, $d = 1 - \delta$, ($\delta \ll 1$) and $d = 1/2$. It is seen that for a duty factor $< 90\%$, local oscillator performance equal to that of the ion standard (for a measuring time τ equal to the period t_d of the sampling cycle) will significantly degrade the characteristic $\tau^{-1/2}$ passive atomic standard performance. For d near 1, ($\delta = (1 - d) \ll 1$) an approximately linear dependence of this degradation on δ is found.

INTRODUCTION

We present the results of calculations which show in detail the effect of local oscillator fluctuations on the long-term stability of those passive atomic frequency standards where the process of atomic line interrogation induces a time-varying sensitivity to frequency fluctuations of the local oscillator. Most notably, this analysis applies to Trapped Ion frequency standards in which the optical sensing signal and the microwave interrogation signal are applied in a cyclical manner. It also necessarily applies to the single-ion optical standards which offer a prospect of dramatic improvements over presently available frequency sources. This work is a part of the Trapped Hg Ion frequency standard development project at JPL, and examples are developed specifically for this particular standard.

The standards under consideration employ a local oscillator (L.O.) to provide the frequency reference for a low-noise microwave interrogation signal. The response of the atoms or ions to this microwave signal is used to generate a feedback signal to correct the frequency of

* This work represents the results of one phase of research carried out at the Jet Propulsion Laboratory, California Institute of Technology, under contract sponsored by the National Aeronautics and Space Administration.

the L.O. This corrected L.O. output is taken as the output signal of the atomic standard itself, and any errors in the feedback process thus degrade the quality of the standard. We show that local oscillator phase noise combines with periodic variation in loop gain to introduce long term fluctuations in this feedback signal.

The calculations have three aspects. First, the time variation of the discriminator sensitivity is derived for single- and double-pulse interrogation of the quantum mechanical transition used to stabilize the L.O. Secondly, a formalism is developed which demonstrates the down-conversion of phase noise in the locked local oscillator by periodic variation of the feedback gain. Finally, these are combined to calculate the effect of a local oscillator on standard performance for various interrogation conditions.

It should be noted that these effects have a very different character from those previously studied effects of local oscillator fluctuations on atomic standard stability which are due to finite loop gain^[1]. The effects calculated here depend crucially on the short-term stability and phase noise of the L.O., rather than on its long-term performance. Furthermore, the resulting degradation of performance continues to much longer measuring times, since the resulting "white" frequency noise has the same character as the statistical limit to the performance of the atomic standard itself.

GENERAL FEATURES

A block diagram of a Trapped-Ion frequency source is shown in Figure 1. Measurement procedure typically involves a sequence of operations to^[2]: 1) Add ions to make up any that have been lost; 2) Pump them completely into the lowest hyperfine level by illumination with the appropriate ultra-violet radiation; 3) Interrogate the ions with a microwave signal which excites approximately half of them from the ground state to an excited state and; 4) Induce fluorescence in the excited ions by illuminating them again. The resulting fluorescent photons are detected and counted to obtain an indication of how many ions were, in fact, excited out of the ground state. If the interrogation signal is properly chosen, the high Q of the ionic transition makes the photon count a very sensitive function of the signal frequency. Finally 5) information derived from the count, as transformed by a control algorithm, is used to update the frequency of the L.O. This sequence is repeated indefinitely.

Because of the small number of ions ($\sim 10^6$), the short term performance of Ion standards is strongly limited by statistical fluctuations in the number of detected photons. This performance improves as the square root of the total number of events recorded. The time per measurement is fundamentally limited by the time needed for microwave interrogation, which in turn is determined by the available Q of the ionic transition. Steps 1), 2), and 4) just described involve operations, each of which takes time to complete, which would interfere with microwave interrogation of the ions. The resulting "dead time" degrades the performance by reducing the number of counts available in any given time.

Steps 1), 2), and 4) also represent time during which the feedback signal is necessarily independent of the L.O. Furthermore, the sensitivity of the photon count to the instantaneous L.O. frequency is in general not uniform over the time period of the microwave interrogation. This is particularly true for the case of single pulse interrogation as is commonly used^[2,3]. As we will show, frequency sensitivity tends to zero at both beginning and end of such a pulse, while double-pulse "Ramsey" type excitation shows a sensitivity which is uniform during time period between pulses. This time dependence within the microwave interrogation combines with the "dead time" to characterize the time dependence of the loop gain.

It is easy to see, in qualitative terms, why L.O. fluctuations at frequencies integrally related

to that of this interrogation cycle must give rise to frequency errors. While a sine-wave frequency fluctuation has an average value of zero, its effect will generally not be zero, since it is detected only some of the time. The feedback loop will then, incorrectly, compensate for the perceived error, offsetting the L.O. from the Ionic transition. Fluctuations near, but not exactly equal to, harmonics of the interrogation frequency f_d are similarly converted to low frequency fluctuations, so long as the loop gain is larger than unity for the difference in frequency. This must be the case for all frequencies of interest, because performance at long times is only improved (over that of the L.O.) by the strength of the loop gain.

It is apparent that noise contribution due to each harmonic of f_i acts independently and that each contributes white noise at offset frequencies (f) very near $f = 0$. This follows from the fact that, while the spectral density of fluctuations for the L.O. $S_y^{LO}(f)$ may be strongly frequency dependent, in a narrow range around each harmonic of f_d , it can be approximated by a constant value. Each of these narrow bands is transformed to a range about zero frequency with an efficiency which we will calculate. From this it follows that the L.O. phase noise performance at high offset frequencies may dominate its effect on the Ion standard's performance. It also follows that the Allan variance of the limiting performance due to this effect (white frequency noise) will have the same $\tau^{-1/2}$ time dependence as that of the standard itself.

In order to compensate for drifts in lamp intensity, ion number, etc. it is necessary to alternately use two different types of microwave interrogation which result in inverted sensitivities of the count to frequency variations. The drift is then cancelled by taking differences between adjacent counts as the raw data for the control loop^[2,3]. This feature does not impact present considerations except for effects such as (e.g.) asymmetrical line shape. Because of the very high Q ($\sim 10^{10}$) of the atomic line and the absence of nearby transitions, such asymmetry is small. By comparison, the other variations which we consider involve large (up to 100%) sensitivity variation.

TIME DEPENDENCE OF THE FREQUENCY SENSITIVITY

Assuming that the atoms or ions are entirely in the ground state, our task is to calculate the instantaneous sensitivity of the final occupation number to frequency over the time period of the microwave interrogation. Since an instantaneous frequency pulse gives rise to a step in phase, this problem reduces to that of sensitivity to an infinitesimal phase step in the microwave exciting signal.

The processes which determine the rate of excitation of atoms or ions from a one energy state to another are explicitly quantum-mechanical. Following Kusch and Hughes^[4] we find the time dependence of phase and amplitude for the excited state wave function by a magnetic spin flip analogue. In this analogue as depicted in Fig. 2a, a vertical magnetic field H_0 generates the energy difference between "down" and "up" states, and a transverse microwave field H_1 is approximately tuned to the precession rate. Transformation to a rotating reference frame at the microwave frequency removes the rapid time variation due to spin precession and allows a simple calculation of the three-dimensional spin orientation as a function of time. In this context, a slight detuning of the microwave frequency ω_1 is represented by incomplete cancellation of H_0 . The time dependent quantum mechanical solutions are simply (slow) precessions of the magnetic moment I about the effective field H_e at an angular rate ω_e which is proportional to the magnitude of that field.

The nature of the computation to be performed is clarified by identifying the field vectors by the frequencies to which they correspond as shown in Figure 2b. All vectors lie in the plane, including the starting position of the moment labeled I , a fact which makes the algebraic relationships between the various frequencies apparent. In its (three-dimensional) precession about ω_e , the vertical component of I depicts the fractional occupation of lower

and upper states, and its horizontal precession angle is determined by the instantaneous phase of the upper state referred to the lower.

Single Pulse Excitation

Figure 3 shows three-dimensional pictures of the precession of I for the case of a π pulse on resonance; and the effect of the same pulse when mistuned to such an extent that exactly half of the ions or atoms are excited. Choosing the microwave amplitude to completely invert the moment within the interrogation time (π pulse) at resonance ($\Delta = 0$) implies

$$\omega_1 \equiv \omega_\pi = \frac{\pi}{t_i} \quad (1)$$

where t_i is the interrogation time. Mistuning to the half signal point corresponds to experimental practice and approximates the condition of maximum slope.

Given the Euler matrices for solid body rotations:

$$r_z(\alpha) = \begin{bmatrix} \cos(\alpha) & \sin(\alpha) & 0 \\ -\sin(\alpha) & \cos(\alpha) & 0 \\ 0 & 0 & 1 \end{bmatrix}, \quad (2)$$

$$r_y(\beta) = \begin{bmatrix} \cos(\beta) & 0 & -\sin(\beta) \\ 0 & 1 & 0 \\ \sin(\beta) & 0 & \cos(\beta) \end{bmatrix}, \quad (3)$$

we define a rotation operator

$$\text{rot}(\theta, \alpha) = r_y(\theta)r_z(\alpha)r_y(-\theta) \quad (4)$$

which generates a rotation by an angle α about ω_e . With unity magnitude initially downward, I is transformed to:

$$\text{rot}(\theta, \alpha) \begin{bmatrix} 0 \\ 0 \\ -1 \end{bmatrix} \quad (5)$$

From Figure 2 we find:

$$\begin{aligned} \theta(\Delta) &= \pi/2 + \arctan\left(\frac{\Delta}{\omega_\pi}\right) \\ &= \pi/2 + \arctan\left(\frac{\Delta t_i}{\pi}\right). \end{aligned} \quad (6)$$

The total angle Ω over which rotation takes place depends on the nature of the pulse and on the frequency offset, Δ . For a π pulse its value is given by (see Fig. 2).

$$\Omega(\Delta) = \pi \sqrt{1 + \left(\frac{\Delta t_i}{\pi}\right)^2}. \quad (7)$$

The net imbalance between upper and lower states at the end of the pulse is given by the Z component of this rotated I :

$$n(\Delta) = \frac{N_{\text{upper}} - N_{\text{lower}}}{N_{\text{total}}} = \begin{bmatrix} 0 \\ 0 \\ 1 \end{bmatrix}^\dagger \text{rot}(\Delta, r(\Delta)) \begin{bmatrix} 0 \\ 0 \\ -1 \end{bmatrix} \quad (8)$$

While expressed somewhat differently, this expression is identical to that given for transition probabilities by Kusch and Hughes^[4]. The frequency offset is found by numerically solving:

$$n(\Delta) = 0, \quad (9)$$

which returns $\Delta = .798685\pi/t_i$, a value slightly different from $\Delta = .761052\pi/t_i$ found for the condition of maximum slope. While the bandwidth is commonly used to characterize the "Q" of the interrogation process, the slope, $dn(\Delta)/d\Delta$ more properly characterizes its discriminating power. Values for this slope (sensitivity to L.O. frequency) are given by $dn(\Delta)/d\Delta = 0.60386t_i$ at $n = 0$, and $0.60553t_i$ for the condition of maximum slope.

Calculation of the instantaneous frequency sensitivity with time is performed as follows: Given the identity of a frequency pulse and phase step as previously discussed, we perform a partial rotation of I about ω_e corresponding to the time before the frequency pulse which we wish to characterize. This is followed by an infinitesimal rotation about the Z axis, corresponding to a phase step in the L.O. A second partial rotation completes a transformation as shown (except for the phase step) in Figs. 3b and 3c. The final value for n is found by projecting the Z component, and a derivative taken with respect the small rotation value.

The sensitivity of the final (approximately zero) value of n to a small phase step, x , taken a time t after the pulse begins is then written

$$g(t) = \lim_{x \rightarrow 0} \begin{bmatrix} 0 \\ 0 \\ 1 \end{bmatrix}^\dagger \text{rot}(\theta, \Omega_2(t)) r_z(x) \text{rot}(\theta, \Omega_1(t)) \begin{bmatrix} 0 \\ 0 \\ -1 \end{bmatrix} \quad (10)$$

with $\Omega_2(t) = \Omega \cdot (1 - (\frac{t}{t_i}))$, and $\Omega_1(t) = \Omega \cdot (\frac{t}{t_i})$.

This somewhat formidable expression reduces to:

$$g(t) = \sin^2(\theta) \cos(\theta) [\sin(\Omega_1(t))(1 - \cos(\Omega_2(t))) + \sin(\Omega_2(t))(1 - \cos(\Omega_1(t)))] \quad (11)$$

which is plotted in Figure 4 for the case $n = 0$. This instantaneous evaluation of fractional occupation number change per radian can be integrated over the pulse length t_i to obtain the overall sensitivity to L.O. frequency. Doing so (again for $n = 0$) yields:

$$G = \int_0^{t_i} g(t) dt = 0.60386t_i; \quad (12)$$

identical to the slope as evaluated earlier.

Double Pulse Excitation

We treat this type of excitation as a phase shift between pulses rather than a frequency offset which generates the phase shift during the time between pulses. We do this, in part, because of the ease of implementation of (nearly) perfectly asymmetric phase shifts necessary for drift compensation. Short $\pi/2$ pulses at the resonance frequency begin and end the interrogation, with the microwave phase shifted by $\pi/2$ radians for the latter. In this case, since the applied frequency is exactly on the resonance, the effective field H_{eff} in Fig. 2a coincides with H_1 . The first pulse rotates the vector I (initially downward) up into the horizontal plane, and the second, with its phase shifted so that H_{eff} points almost exactly along (or away) from I , shifts it out of the plane only to the extent of any misalignment. Any frequency error in the L.O. will result in such a misalignment.

It is apparent that a L.O. phase step at any time between the pulses will have the same effect as at any other time, since the effect of either one of them on the phase during the final pulse is the same. For these conditions, a calculation similar to that for the single pulse gives dependencies for the three time intervals as:

$$\begin{aligned} g(t) &= \sin(\pi t / 2t_p) & 0 > t > t_p, \\ &= 1 & t_p < t < t_i - t_p, \\ &= \sin(\pi \frac{t_i - t_p}{2t_p}) & t_i - t_p < t < t_i, \end{aligned} \quad (13)$$

where t_p is the short pulse time, and t_i the interrogation time as before. Figure 5 shows the resulting sensitivity over the interrogation cycle for $t_p = 0.1t_i$. A comparison to Figure 4 shows that the sensitivity is much more nearly constant in time during the actual microwave interrogation. As we show in the following section, if the "dead time" between interrogations were made small, this could have a major impact on L.O. requirements.

A related comparison to the case of a single pulse can be found by integrating the value of this sensitivity over the time t_i to obtain

$$G = \int_0^{t_i} g(t) dt = t_i - \frac{4}{\pi} t_p. \quad (14)$$

In the limit of narrow pulses, a comparison to Eq. [12] shows an improvement in discriminating power, or effective Q, of $1/0.603864 = 1.6560$ over single pulse excitation. This is a slightly larger improvement factor than that given by the reduction in bandwidth: $0.798685/.5 = 1.5974$.

PHASE NOISE DOWNCONVERSION

A simplified block diagram of the frequency-locked loop is shown in Figure 6. Here the time dependence of the sensitivity of the measured atomic transition rate is combined with the microwave duty cycle to give an effective time dependent modulation $g(t)$ of the loop gain as shown. In this model, frequency noise $S_y^{LO}(f)$ in the Local Oscillator as partially compensated by feedback from the Integrator results in Signal Output from the locked local oscillator with frequency fluctuations $S_y^{LLO}(f)$. Compensation to achieve high long term stability is accomplished by a feedback circuit in which the Signal Output frequency fluctuations are first converted into voltage fluctuations $S_v^d(f)$ by the action of a high Q Discriminator and then to $S_v^m(f)$ by the action of the Modulator. This voltage is then integrated to provide a correction to the frequency of the Local Oscillator.

We identify a time constant t_i for the Integrator which is more properly characteristic of the entire loop; assuming that for $f \gg t_i/2\pi$ the loop gain is approximately zero, while for $f \ll t_i/2\pi$ the loop gain is much greater than unity. Thus, high frequency fluctuations will be uncompensated by the action of the loop, so that $S_y^{LLO}(f) = S_y^{LO}(f)$ for $f \gg t_i/2\pi$. However, low frequency fluctuations, as detected, are nearly completely compensated. From these two conditions it follows that any down-conversion of high frequency components of $S_v^d(f)$ to low frequency components in $S_v^m(f)$ will result in an identical transformation in the locked loop between $S_y^{LO}(f)$ and $S_y^{LLO}(f)$ subject only to requirements on "high" and "low" frequency given above.

Depending on the harmonic content of $g(t)$, the Modulator will introduce such down-conversion for "high" frequencies very near integral multiples of $f_d = 1/t_d$ to frequencies near $f = 0$. Frequency requirements can thus be satisfied by assuming $t_d \ll t_i \ll \tau$, where τ is the time over which the stability of the Signal Output is measured. Depending on the

average value of $g(t)$, the Modulator passes feedback signals near $f = 0$. Choosing the phase by symmetry, the coefficients g_n for amplitude conversion near the n th harmonic of f_d can be written:

$$g_n = \int_0^{t_d} g(t) \cos\left(\frac{2\pi n t}{t_d}\right) dt, \quad (15)$$

while the average value g_0 is:

$$g_0 = \int_0^{t_d} g(t) dt. \quad (16)$$

Assuming complete compensation by the loop for the down-converted fluctuations, "white" noise in the narrow range about each harmonic, and taking into account fluctuations at frequencies both above and below harmonics $n f_d$, the low frequency contribution to $S_y^{LLO}(f)$ is given by

$$g_0^2 S_y^{LLO}(0) = 2 \cdot \sum_{n=1}^{\infty} g_n^2 S_y^{LO}(n f_d). \quad (17)$$

The consequences of this relation depend in detail on the nature of the noise which characterizes the local oscillator and on the time dependence of the duty factor. If, for example, L.O. noise increases rapidly with frequency, the sum may not converge. We find this to be the case for white phase noise, which characterizes the Hydrogen maser over much of its useful range, under double pulse conditions as described below. Fortunately, Quartz crystal oscillators show better behavior.

Modeling Quartz oscillator performance by a flat Allan variance σ_q over the time range of interest (see Fig. 7) allows its flicker frequency noise to be calculated as^[5]

$$S_y^{LO}(f) = \frac{1}{2 \ln(2)} \frac{\sigma_q^2}{f}. \quad (18)$$

Correspondingly, the limiting Ion Standard variance as measured at cycle time t_d can be related to the white noise of the locked loop $S_y^{LLO}(0)$ by

$$\sigma_d^2 = \frac{S_y^{LLO}(0)}{2 t_d}. \quad (19)$$

Combining Equations 17, 18 and 19 allows us to calculate a performance ratio S_d as shown in Fig. 7 between the limiting Ion performance at the cycle time and the (constant) Quartz oscillator performance given by

$$S_d^2 \equiv \frac{\sigma_d^2}{\sigma_q^2} = \frac{1}{2 \ln(2)} \frac{1}{g_0^2} \sum_{n=1}^{\infty} \frac{g_n^2}{n}. \quad (20)$$

We have calculated the performance ratio $S_d(d)$ given in Eq [20] for single pulse excitation and for double pulse excitation assuming two infinitely narrow pulses. Frequency sensitivity during microwave interrogation is assumed to be as shown in Fig. 4 for single pulse excitation, and to be a constant for the double pulse case. Both cases were evaluated by means of numerical techniques over a fairly wide range for the duty factor d . In addition, limiting forms were derived for double pulse interrogation for both high and low duty factors. Results of these calculations are shown in Figures 8 and 9.

Figure 8 shows that, for duty factors significantly less than unity, little difference in local oscillator performance requirements can be expected between single and double pulse cases. For a 50% duty factor, values for S_d are .71 and .55 respectively. That is, for this typical

case, the limiting stability of the Ion standard as measured at the cycle time is 1 1/2 to 2 times below that of the Quartz reference.

Performance ratios for duty factors near unity are shown in Figure 9. For very small values of $\delta = 1-d$, a very different picture emerges. Here a limiting value of $S_d = .305$ is reached with single pulse excitation, while the use of two pulses allows substantially reduced sensitivity to the local oscillator. This reduction demonstrates a smooth transition to the case of continuous excitation, which shows no such sensitivity to the local oscillator.

CONCLUSIONS

A critical requirement on local oscillator performance is presented which has not been previously evaluated. It is not characteristic of continuously excited passive atomic sources but is rather unique to new standards using a cyclical excitation and interrogation cycle. For typical Trapped Ion frequency standards, it places requirements on local oscillator performance which are approximately equal to that of the standard itself at the interrogation time. Reduced requirements may result from the use of double pulse interrogation and very high duty factors.

Since Quartz oscillator performance better than $\Delta f/f = 10^{-12}$ is easily obtained, present Trapped Ion standards, with stabilities in the low $10^{-12}/\sqrt{\tau}$ range and cycle times of seconds, do not require improved local oscillators. However, orders of magnitude of improvement are projected for both trapped ion and single ion (optical) standards. Local oscillator requirements critical to this performance could probably not be met by presently available oscillators.

ACKNOWLEDGEMENTS

The author would like to express his gratitude to J. Prestage and C. Greenhall for their substantial contributions to the Quantum Mechanical and Mathematical aspects of this work. He would also like to thank R.L. Sydnor for encouragement and help, L. Maleki for his insight and many contributions, and L. Cutler for pointing out the problem.

APPENDIX

Calculation of limiting forms

Double pulse excitation with infinitely narrow pulses gives uniform time dependence during the interrogation (see Fig. 5). Substituting $g(t) = 1$ in Equations [15] and [16] gives $g_0 = dt_d$ and

$$g_n = t_d \int_{-d/2}^{d/2} \cos(2\pi n x) dx = t_d \frac{\sin(\pi n d)}{n\pi} \quad (21)$$

which, substituted in Eq [20] gives

$$S_d^2 = \frac{1}{2 \ln(2)} \frac{1}{d^2} \sum_{n=1}^{\infty} \frac{\sin^2(\pi n d)}{\pi^2 n^3}. \quad (22)$$

For small values of d , the sum can be approximated to order d^2 by $d^2(\ln(1/(2\pi d)) + 3/2)^{[6]}$, giving a limiting expression for $d \ll 1$ of

$$S_d^2 = \frac{1}{2 \ln(2)} \left(\ln\left(\frac{1}{2\pi d}\right) + 3/2 \right). \quad (23)$$

It is easy to show that the same integral results for the complementary limiting case $\delta = 1 - d \ll 1$ except that d is replaced by δ . This gives a performance ratio

$$S_d^2 = \frac{1}{2 \ln(2)} \frac{\delta^2}{d^2} \left(\ln\left(\frac{1}{2\pi\delta}\right) + 3/2 \right). \quad (24)$$

Equations [23] and [24] are the limiting forms plotted in Figures 8 and 9, respectively.

REFERENCES

- (1) Vanier, J. et al, "Transfer of Frequency Stability from an Atomic Frequency Reference to a Quartz-Crystal Oscillator," IEEE Trans. Instrum. Meas., Vol. IM-28, 188 (1979)
- (2) Prestage, J.D., Dick, G.J., and Maleki, L., "JPL Trapped Frequency Standard Development," Proc. 41st Ann. Symp. Freq. Control, 20, Philadelphia, Pa., May, 1987. also Prestage, J.D., Dick, G.J., and Maleki, L., this conference.
- (3) Cutler, L.S. et al, "A Trapped Mercury 199 Ion Frequency Standard," Proc. 13th Ann. Precise Time and Time Interval (PTTI) Planning and Applications Meeting, 563 (1981). Wineland, D.J. et al, "Proposed Stored $^{201}\text{Hg}^+$ Ion Frequency Standards," Proc. 35th Ann. Symp. on Freq. Control, 602 (1981). Cutler, L.S., Giffard, R.P., Wheeler, P.J., and Winkler, G.M., "Operational Experience with a Mercury Ion Storage Frequency Standard," Proc. 41st Ann. Symp. on Freq. Control, 12, Philadelphia, Pa., May, 1987.
- (4) Kusch, P. and Hughes, V.W., "Atomic and Molecular Beam Spectroscopy," in "Handbuch der Physik," Ed. S. Flügge, Vol. XXXVII/1, p. 55, (1959).
- (5) "Characterization of Frequency and Phase Noise," Recommendations and Reports of the CCIR, XVth Plenary Session, Report 580-1, 91(1982).
- (6) "Handbook of Mathematical Functions," Ed. M. Abramowitz and I.A. Stegun, Dover Publications, Inc., New York (1964).

FIGURE CAPTIONS

- (1) Schematic Diagram of the Trapped Mercury Ion Frequency Standard.
- (2) Field and Frequency diagrams for spin with moment I in rotating reference system.
- (3) Three dimensional views of path of moment I on and off resonance.
- (4) Time dependence of sensitivity to local oscillator frequency for a single π pulse detuned to point of half maximum response.
- (5) Time dependence of sensitivity to local oscillator frequency for double $\pi/2$ pulse excitation (see text).
- (6) Simplified block diagram used as basis for calculations.
- (7) Corresponding performance for Quartz local oscillator and Trapped Ion standard identifying Variance Ratio at cycle time.
- (8) Variance Ratio for small Duty Factor.
- (9) Variance Ratio for Duty Factor near unity.

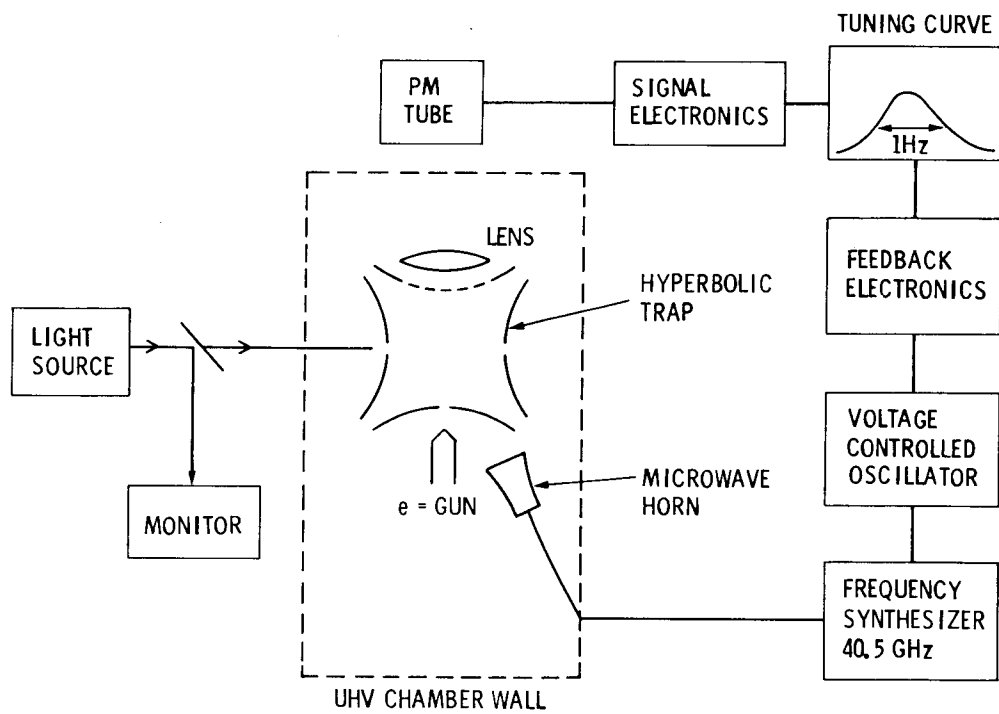


Figure 1 Schematic Diagram of the Trapped Mercury Ion Frequency Standard.

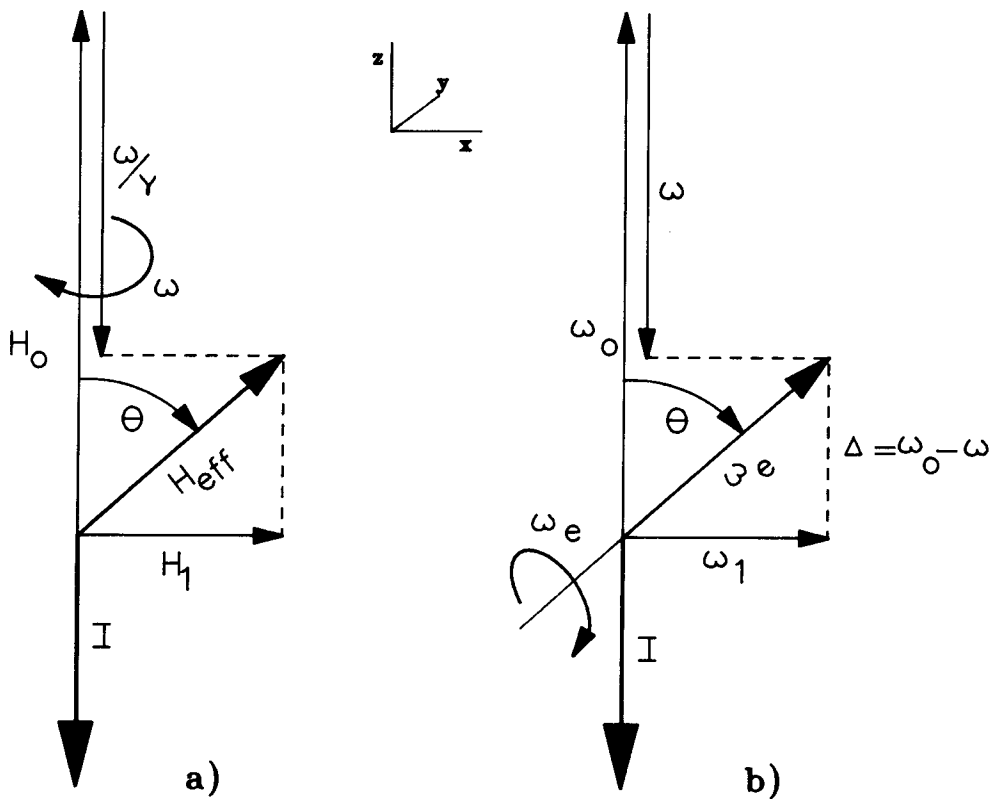


Figure 2 Field and Frequency diagrams for magnetic moment I in rotating reference system.

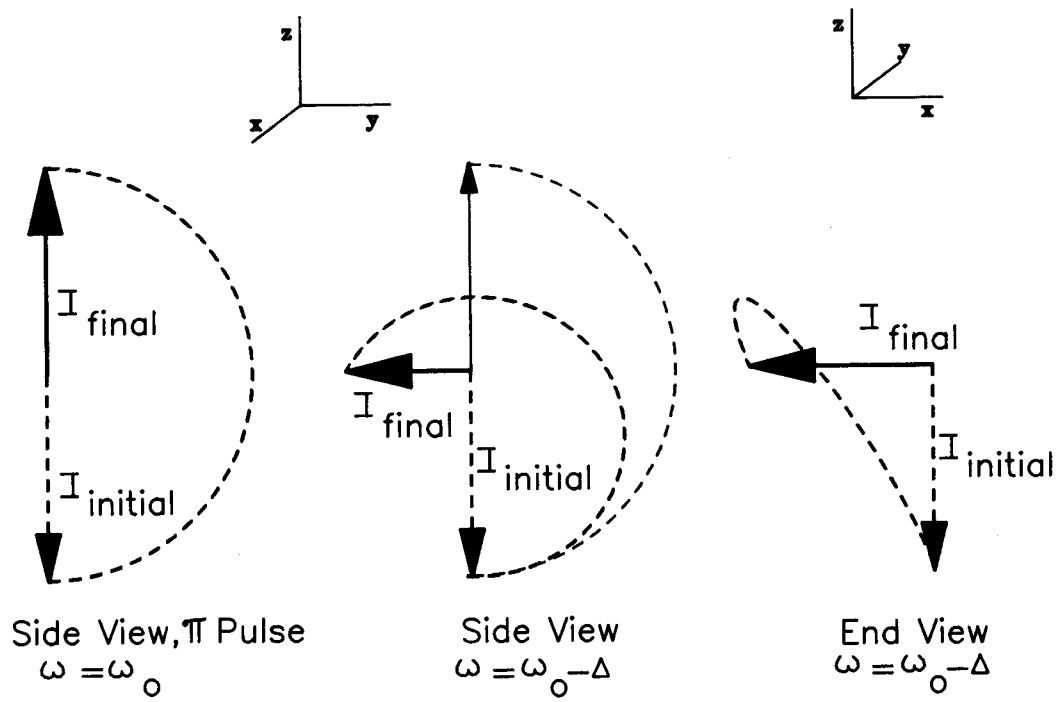


Figure 3 Three dimensional views of path of moment \mathbf{I} on and off resonance.

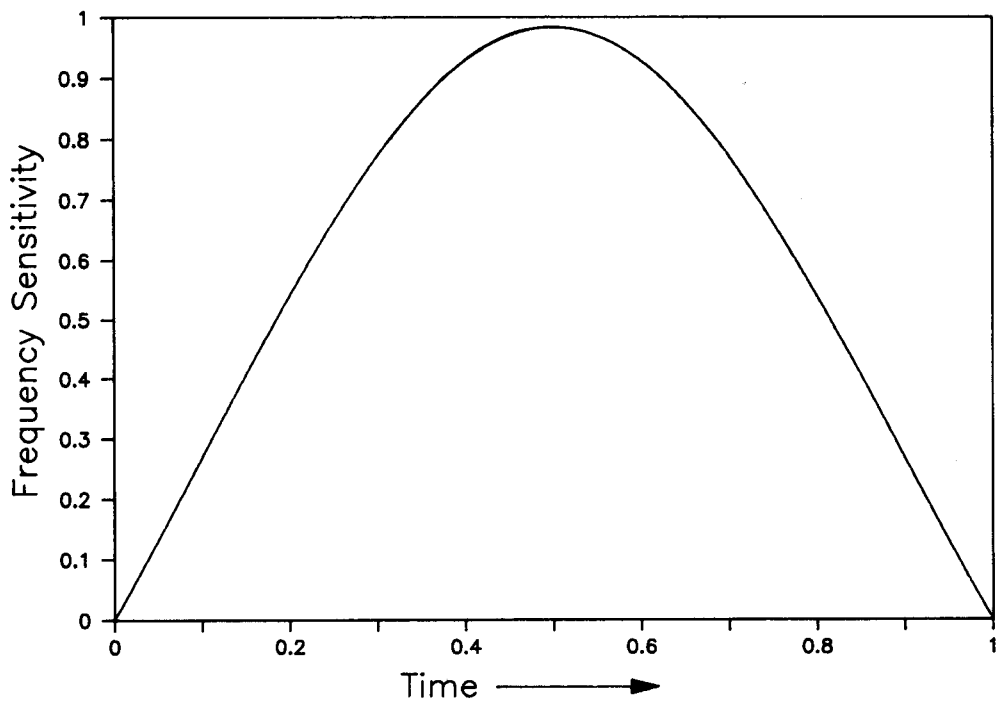


Figure 4 Time dependence of sensitivity to local oscillator frequency for a single π pulse detuned to point of half maximum response.

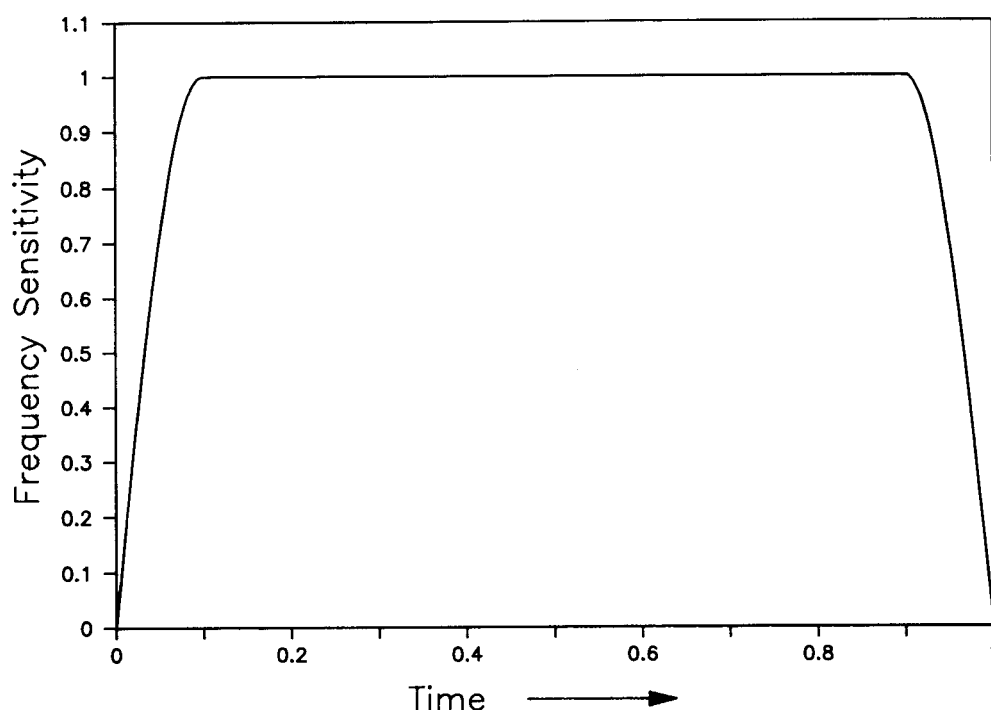


Figure 5 Time dependence of sensitivity to local oscillator frequency for double $\pi/2$ pulse excitation (see text).

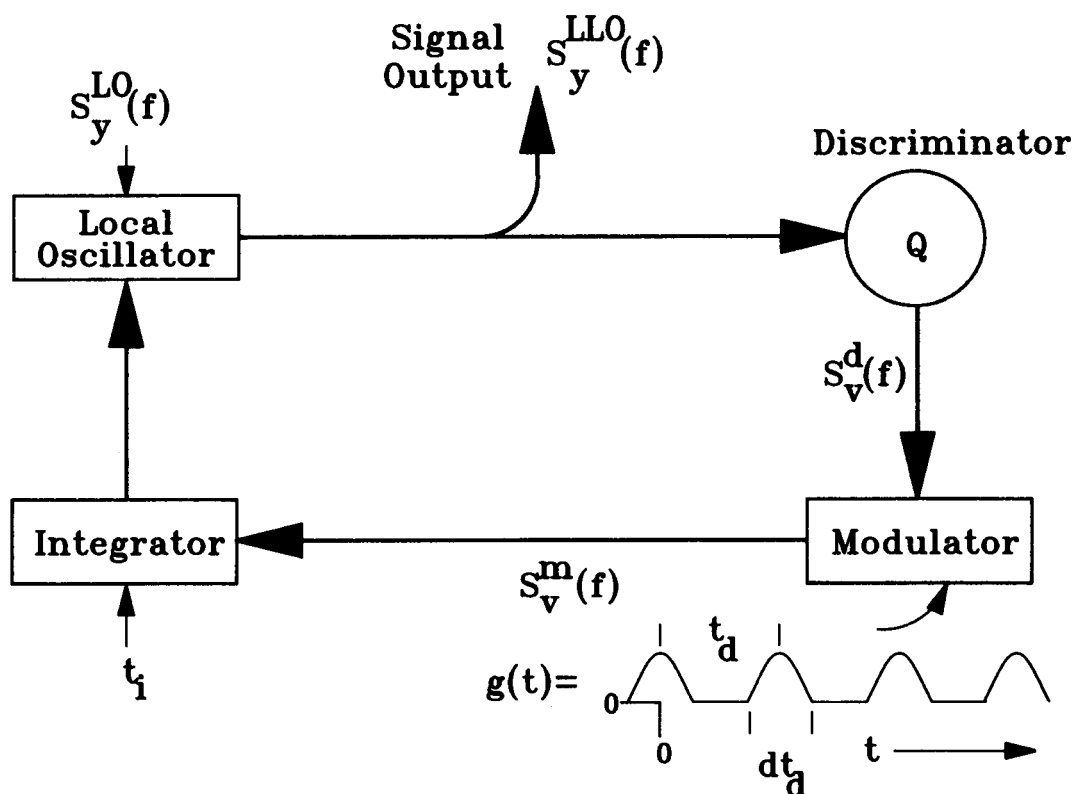


Figure 6 Simplified block diagram used as basis for calculations.

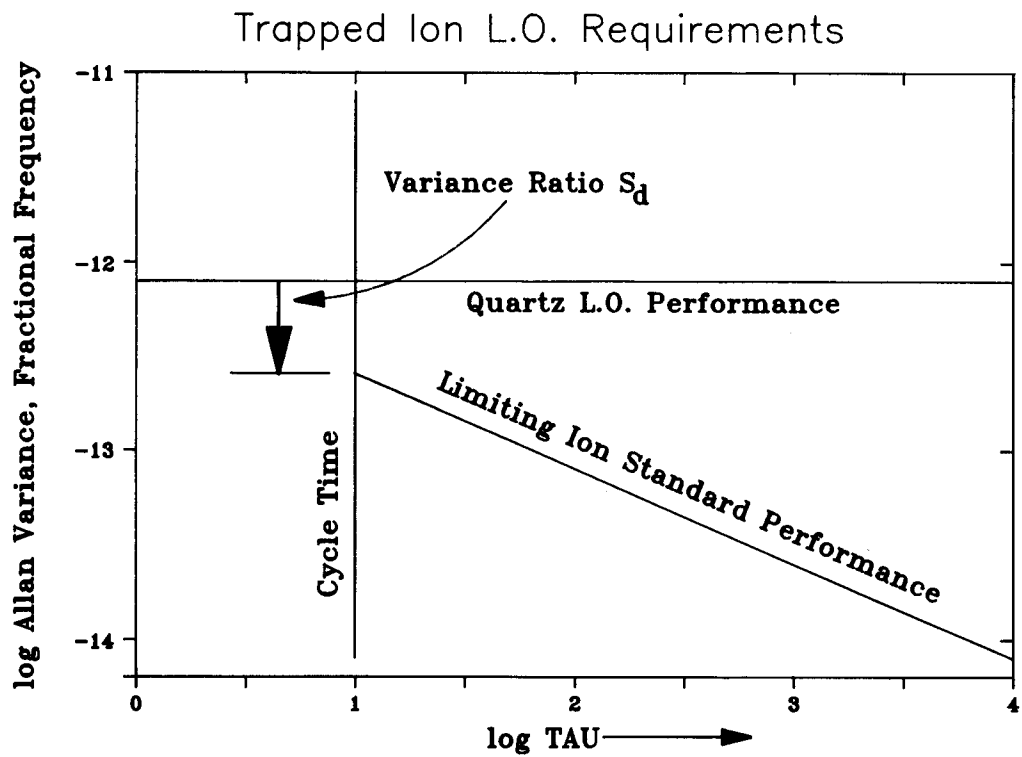


Figure 7 Correspond performance for Quartz local oscillator and Trapped Ion Standard identifying Variance Ratio at cycle time.

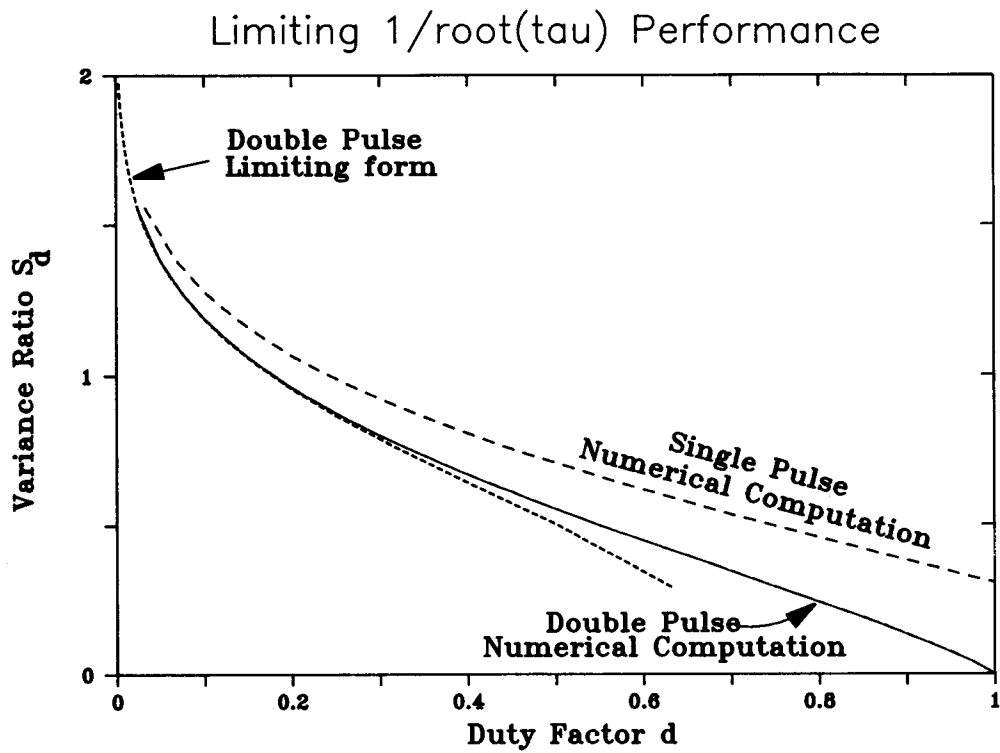


Figure 8 Variance Ratio for small Duty factor.

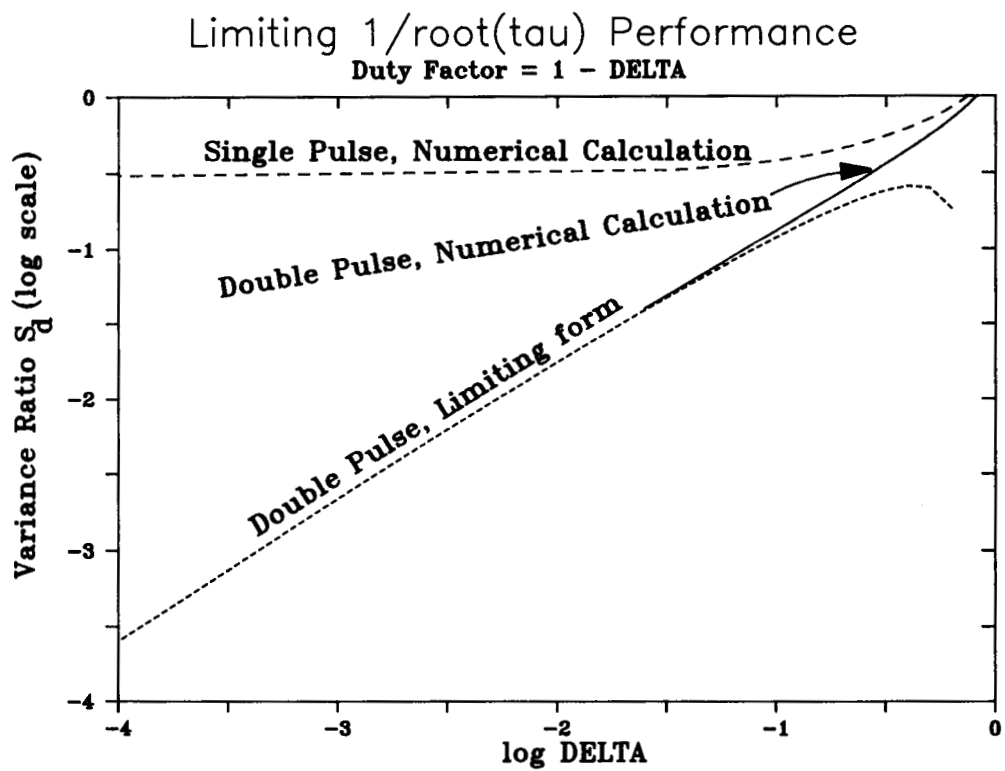


Figure 9 Variance Ratio for Duty factor near unity.